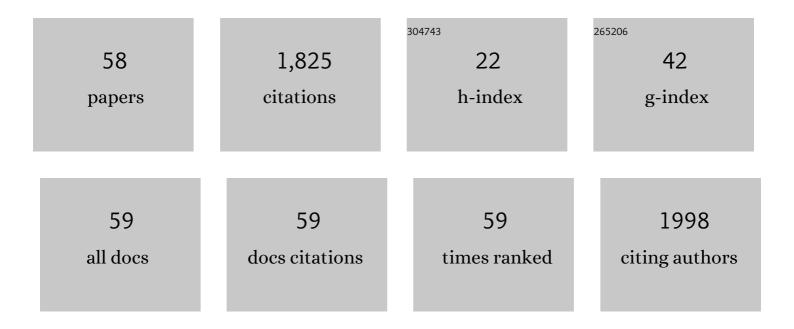
List of Publications by Year in descending order

Source: https://exaly.com/author-pdf/4057671/publications.pdf Version: 2024-02-01



#	Article	IF	CITATIONS
1	Scanning Tunneling Microscopy of Metal Phthalocyanines:Â d7and d9Cases. Journal of the American Chemical Society, 1996, 118, 7197-7202.	13.7	359
2	Scanning Tunneling Microscopy, Orbital-Mediated Tunneling Spectroscopy, and Ultraviolet Photoelectron Spectroscopy of Metal(II) Tetraphenylporphyrins Deposited from Vapor. Journal of the American Chemical Society, 2001, 123, 4073-4080.	13.7	246
3	Kinetic and thermodynamic processes of organic species at the solution–solid interface: the view through an STM. Chemical Communications, 2015, 51, 4737-4749.	4.1	93
4	Single Molecule Imaging of Oxygenation of Cobalt Octaethylporphyrin at the Solution/Solid Interface: Thermodynamics from Microscopy. Journal of the American Chemical Society, 2012, 134, 14897-14904.	13.7	83
5	Orbital Mediated Tunneling in Vanadyl Phthalocyanine Observed in both Tunnel Diode and STM Environments. Journal of Physical Chemistry B, 2000, 104, 2444-2447.	2.6	75
6	New Nanoscale Insights into the Internal Structure of Tetrakis(4-sulfonatophenyl) Porphyrin Nanorods. Journal of Physical Chemistry C, 2009, 113, 1709-1718.	3.1	71
7	Differing HOMO and LUMO Mediated Conduction in a Porphyrin Nanorod. Journal of the American Chemical Society, 2010, 132, 8554-8556.	13.7	66
8	A Single Molecule Level Study of the Temperature-Dependent Kinetics for the Formation of Metal Porphyrin Monolayers on Au(111) from Solution. Journal of the American Chemical Society, 2014, 136, 2142-2148.	13.7	61
9	Effect of dispersion on surface interactions of cobalt( <scp>ii</scp> ) octaethylporphyrin monolayer on Au(111) and HOPG(0001) substrates: a comparative first principles study. Physical Chemistry Chemical Physics, 2014, 16, 14096-14107.	2.8	58
10	Correlating elastic properties and molecular organization of an ionic organic nanostructure. Nanoscale, 2014, 6, 316-327.	5.6	45
11	A Self-Assembled Two-Dimensional Zwitterionic Structure: H <sub>6</sub> TSPP Studied on Graphite. Journal of Physical Chemistry C, 2011, 115, 3990-3999.	3.1	38
12	Kinetic and Thermodynamic Control in Porphyrin and Phthalocyanine Self-Assembled Monolayers. Langmuir, 2018, 34, 3-17.	3.5	37
13	Resonant Tunneling in Metal Phthalocyanines. The Journal of Physical Chemistry, 1994, 98, 8169-8172.	2.9	33
14	Temperature Stability of Three Commensurate Surface Structures of Coronene Adsorbed on Au(111) from Heptanoic Acid in the 0 to 60 °C Range. Journal of Physical Chemistry C, 2013, 117, 2914-2919.	3.1	32
15	Comprehensive structure–function correlation of photoactive ionic π-conjugated supermolecular assemblies: an experimental and computational study. Journal of Materials Chemistry C, 2016, 4, 10223-10239.	5.5	32
16	Kinetically Trapped Two-Component Self-Assembled Adlayer. Journal of Physical Chemistry C, 2015, 119, 25364-25376.	3.1	27
17	Desorption Kinetics and Activation Energy for Cobalt Octaethylporphyrin from Graphite at the Phenyloctane Solution–Graphite Interface: An STM Study. Journal of Physical Chemistry C, 2015, 119, 9386-9394.	3.1	26
18	A Systematic Approach toward Designing Functional Ionic Porphyrin Crystalline Materials. Journal of Physical Chemistry C, 2018, 122, 22803-22820.	3.1	25

#	Article	IF	CITATIONS
19	Spontaneous Solution-Phase Redox Deposition of a Dense Cobalt(II) Phthalocyanine Monolayer on Gold. Journal of Physical Chemistry B, 2004, 108, 17003-17006.	2.6	24
20	Charge transfer induced chemical reaction of tetracyano-p-quinodimethane adsorbed on graphene. RSC Advances, 2012, 2, 10579.	3.6	24
21	Solvent-Induced Variations in Surface Structure of a 2,9,16,23-Tetra-tert-butyl-phthalocyanine on Graphite. Journal of Physical Chemistry C, 2009, 113, 17479-17483.	3.1	23
22	Hyperbranched crystalline nanostructure produced from ionic π-conjugated molecules. Chemical Communications, 2015, 51, 2663-2666.	4.1	23
23	Surface directed reversible imidazole ligation to nickel( <scp>ii</scp> ) octaethylporphyrin at the solution/solid interface: a single molecule level study. Physical Chemistry Chemical Physics, 2016, 18, 20819-20829.	2.8	23
24	Predicting the Size Distribution in Crystallization of TSPP:TMPyP Binary Porphyrin Nanostructures in a Batch Desupersaturation Experiment. Crystal Growth and Design, 2014, 14, 6599-6606.	3.0	22
25	Influence of the Central Metal Ion on the Desorption Kinetics of a Porphyrin from the Solution/HOPG Interface. Journal of Physical Chemistry C, 2016, 120, 18140-18150.	3.1	18
26	Structure, Properties, and Reactivity of Porphyrins on Surfaces and Nanostructures with Periodic DFT Calculations. Applied Sciences (Switzerland), 2020, 10, 740.	2.5	18
27	Protonation state of core nitrogens in the <i>meso</i> -tetra(4-carboxyphenyl)porphyrin impacts the chemical and physical properties of nanostructures formed in acid solutions. Journal of Porphyrins and Phthalocyanines, 2012, 16, 1233-1243.	0.8	17
28	Resonance Raman Spectroscopy of Helical Porphyrin Nanotubes. Journal of Physical Chemistry C, 2010, 114, 16357-16366.	3.1	16
29	Amorphous or nanocrystalline AlN thin films formed from AlN: H. Journal of Materials Research, 1994, 9, 1449-1455.	2.6	15
30	Polymorphic, Porous, and Host–Guest Nanostructures Directed by Monolayer–Substrate Interactions: Epitaxial Self-Assembly Study of Cyclic Trinuclear Au(I) Complexes on HOPG at the Solution–Solid Interface. Journal of Physical Chemistry C, 2015, 119, 24844-24858.	3.1	15
31	Tuning the optoelectronic characteristics of ionic organic crystalline assemblies. Journal of Materials Chemistry C, 2018, 6, 4041-4056.	5.5	15
32	Highly ordered thin films prepared with octabutoxy copper phthalocyanine complexes. Ultramicroscopy, 2003, 97, 271-278.	1.9	14
33	Nanomechanical properties of ordered phthalocyanine Langmuir–Blodgett layers. Journal of Materials Research, 2004, 19, 1461-1470.	2.6	14
34	Electron affinity states of metal supported phthalocyanines measured by tunneling spectroscopy. Journal of Porphyrins and Phthalocyanines, 2012, 16, 273-281.	0.8	14
35	Structural and Electronic Properties of Columnar Supramolecular Assemblies Formed from Ionic Metal-Free Phthalocyanine on Au(111). Journal of Physical Chemistry C, 2011, 115, 16305-16314.	3.1	12
36	Photoconductive behavior of binary porphyrin crystalline assemblies. Journal of Porphyrins and Phthalocyanines, 2017, 21, 569-580.	0.8	12

#	Article	IF	CITATIONS
37	Cooperativity and coverage dependent molecular desorption in self-assembled monolayers: computational case study with coronene on Au(111) and HOPG. Physical Chemistry Chemical Physics, 2019, 21, 10505-10513.	2.8	11
38	Balancing Noncovalent Interactions in the Self-Assembly of Nonplanar Aromatic Carboxylic Acid MOF Linkers at the Solution/Solid Interface: HOPG vs Au(111). Langmuir, 2019, 35, 5271-5280.	3.5	11
39	STM Investigation of the Y[C6S-Pc]2 and Y[C4O-Pc]2Complex at the Solution–Solid Interface: Substrate Effects, Submolecular Resolution, and Vacancies. Journal of Physical Chemistry C, 2021, 125, 1421-1431.	3.1	10
40	A new variable temperature solution-solid interface scanning tunneling microscope. Review of Scientific Instruments, 2014, 85, 103701.	1.3	9
41	Functional Porphyrin Nanostructures for Molecular Electronics: Structural, Mechanical, and Electronic Properties of Self-Assembled Ionic Metal-Free Porphyrins. , 2016, , 69-103.		8
42	Cooperative Binding of 1-Phenylimidazole to Cobalt(II) Octaethylporphyrin on Graphite: A Quantitative Imaging and Computational Study at Molecular Resolution. Journal of Physical Chemistry C, 2020, 124, 18639-18649.	3.1	8
43	Scanning Tunneling Microscopy Reveals Surface Diffusion of Single Double-Decker Phthalocyanine Molecules at the Solution/Solid Interface. Journal of Physical Chemistry C, 2022, 126, 4140-4149.	3.1	8
44	Quantifying reversible nitrogenous ligand binding to Co( <scp>ii</scp> ) porphyrin receptors at the solution/solid interface and in solution. Physical Chemistry Chemical Physics, 2020, 22, 24226-24235.	2.8	6
45	Crystallographic STM image processing of 2D periodic and highly symmetric molecule arrays. , 2011, , .		5
46	Single molecule level studies of reversible ligand binding to metal porphyrins at the solution/solid interface. Journal of Porphyrins and Phthalocyanines, 2020, 24, 993-1002.	0.8	5
47	Persistent Conductivity in TPyP:TSPP Organic Nanorods Induced by Ion Bombardment. Journal of Physical Chemistry C, 2016, 120, 14962-14968.	3.1	5
48	Single-Molecule Kinetic Analysis of Oxygenation of Co(II) Porphyrin at the Solution/Solid Interface. Journal of Physical Chemistry Letters, 2022, 13, 4918-4923.	4.6	4
49	Morphology Dependent Conductivity and Photoconductivity of Ionic Porphyrin Crystalline Assemblies. ECS Journal of Solid State Science and Technology, 2020, 9, 061010.	1.8	3
50	Aggregation of sulfonated free-base phthalocyanine on gold as a function of solution pH. Journal of Porphyrins and Phthalocyanines, 2011, 15, 459-466.	0.8	2
51	Mechanical behavior of crystalline ionic porphyrins. Journal of Porphyrins and Phthalocyanines, 2019, 23, 154-165.	0.8	2
52	Role of the Supporting Surface in the Thermodynamics and Cooperativity of Axial Ligand Binding to Metalloporphyrins at Interfaces. Current Organic Chemistry, 2022, 26, 553-562.	1.6	1
53	Resonance Raman Spectroscopy of Helical Porphyrin Nanotubes: Hierarchal Structure and Exciton Coupling. , 2010, , .		0
54	The Role of Solvent in the Hierarchal Structure of a Porphyrin Aggregate. , 2010, , .		0

#	Article	IF	CITATIONS
55	A New variable temperature solution-solid interface scanning tunneling microscope. Microscopy and Microanalysis, 2015, 21, 2187-2188.	0.4	0
56	Structure-Function Correlation of Photoactive Ionic pi-Conjugated Binary Porphyrin Assemblies. MRS Advances, 2017, 2, 2267-2273.	0.9	0
57	Quantifying Reversible Nitrogenous Ligand Binding to Co(II) Porphyrin Receptors at the Solution/Solid Interface and in Solution. ECS Meeting Abstracts, 2021, MA2021-01, 788-788.	0.0	0
58	STM Investigation of Y[C6s-Pc]2 and Y[C4o-Pc]2 Complexes at the Solution/Solid Interface: Substrate Effects, Sub-Molecular Resolution, and Covalently Saturated Sulfur. ECS Meeting Abstracts, 2021, MA2021-01, 787-787.	0.0	0